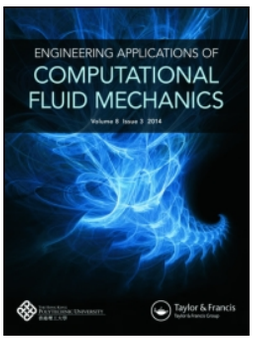

Taylor & Francis
Taylor & Francis Group

Engineering Applications of Computational Fluid Mechanics

ISSN: 1994-2060 (Print) 1997-003X (Online) Journal homepage: https://www.tandfonline.com/loi/tcfm20

Modeling temperature dependency of oil - water relative permeability in thermal enhanced oil recovery processes using group method of data handling and gene expression programming

Nait Amar Menad, Zeraibi Noureddine, Abdolhossein Hemmati-Sarapardeh, Shahaboddin Shamshirband, Amir Mosavi & Kwok-wing Chau

To cite this article: Nait Amar Menad, Zeraibi Noureddine, Abdolhossein Hemmati-Sarapardeh, Shahaboddin Shamshirband, Amir Mosavi & Kwok-wing Chau (2019) Modeling temperature dependency of oil - water relative permeability in thermal enhanced oil recovery processes using group method of data handling and gene expression programming, Engineering Applications of Computational Fluid Mechanics, 13:1, 724-743, DOI: 10.1080/19942060.2019.1639549

To link to this article: https://doi.org/10.1080/19942060.2019.1639549

Published online: 25 Jul 2019.

ENGINEERING APPLICATIONS OF COMPUTATIONAL FLUID MECHANICS
2019, VOL. 13, NO. 1, 724–743
https://doi.org/10.1080/19942060.2019.1639549

Taylor & Francis
Taylor & Francis Group

Modeling temperature dependency of oil - water relative permeability in thermal enhanced oil recovery processes using group method of data handling and gene expression programming

Nait Amar Menad[a], Zeraibi Noureddine[a], Abdolhossein Hemmati-Sarapardeh[b], Shahaboddin Shamshirband[c,d], Amir Mosavi[e,f] and Kwok-wing Chau[g]

[a]Laboratoire Génie Physique des Hydrocarbures, Faculty of Hydrocarbons and Chemistry, University M'hamed Bougara of Boumerdes, Boumerdes, Algeria; [b]Department of Petroleum Engineering, Shahid Bahonar University of Kerman, Kerman, Iran; [c]Department for Management of Science and Technology Development, Ton Duc Thang University, Ho Chi Minh City, Vietnam; [d]Faculty of Information Technology, Ton Duc Thang University, Ho Chi Minh City, Vietnam; [e]Institute of Automation, Kando Kalman Faculty of Electrical Engineering, Obuda University, Budapest, Hungary; [f]School of the Built Environment, Oxford Brookes University, Oxford, UK; [g]Department of Civil and Environmental Engineering, Hong Kong Polytechnic University, Hong Kong, People's Republic of China

ABSTRACT

In the implementation of thermal enhanced oil recovery (TEOR) techniques, the temperature impact on relative permeability in oil–water systems (K_{rw} and K_{ro}) is of special concern. Hence, developing a fast and reliable tool to model the temperature effect on K_{rw} and K_{ro} is still a major challenge for precise studying of TEOR processes. To reach the goal of this work, two promising soft-computing algorithms, namely Group Method of Data Handling (GMDH) and Gene Expression Programming (GEP) were employed to develop reliable and simple to use paradigms to predict the temperature dependency of K_{rw} and K_{ro}. To do so, a large database encompassing wide-ranging temperatures and fluids/rock parameters, was considered to establish these correlations. Statistical results and graphical analyses disclosed the high degree of accuracy for the proposed correlations in emulating the experimental results. In addition, GEP correlations were found to be the most consistent with root mean square error (RMSE) values of 0.0284 and 0.0636 for K_{rw} and K_{ro}, respectively. Lastly, the performance comparison against the preexisting correlations indicated the large superiority of the newly introduced correlations. The findings of this study can help for better understanding the temperature dependency of K_{rw} and K_{ro} in TEOR.

ARTICLE HISTORY
Received 29 April 2019
Accepted 1 July 2019

KEYWORDS
Thermal enhanced oil recovery (TEOR); temperature effect on oil/water relative; GMDH; GEP

1. Introduction

Nowadays, energy demand is expected to rise significantly with the increased prosperity in different sectors of industry and with the higher and continues consumption (Tillerson, 2008). As fossil source is still the dominant spring of energy, there have been noticeable and significant efforts to promote the standards techniques to improve the outcomes from oil reservoirs (Olayiwola & Dejam, 2019). Due to this fact, extraction of oil from unconventional reservoirs and oil with low API gravity has turned into quite important ways to compensate the expected need in the fossil energy (Meyer, Attanasi, & Freeman, 2007). The high amount of heavy oils and bitumen over the worldwide raises awareness on this supplementary source of fossil energy although the deficiencies in the characteristics of associated oil such as the high viscosity, low API gravity, and asphaltene content (Ameli, Alashkar, & Hemmati-Sarapardeh, 2018; Green & Paul Willhite, 1998; Prats, 1982; Saboorian-Jooybari, Dejam, & Chen, 2016). Therefore, one robust procedure to address such extreme conditions is increasing the temperature by means of steam or hot water injection, to reduce the viscosity which represents the resistance to the flow (Prats, 1982). These temperature-based techniques for oil recovery are assembled beneath the umbrella of the so-called Thermal Enhanced Oil Recovery (TEOR).

TOER includes many methods in which the main screening application criterion is based on the viscosity values. Accordingly, we distinguish steam-assisted gravity drainage (SAGD) process that is applied for the recovery of bitumen, steam flooding which is effective for the case of heavy oil extraction and cyclic steam stimulation (CSS) which is appropriate for extra-heavy oil (Ameli et al., 2018). It is well known that in such techniques, temperature has strong influence on the porous medium flow; and hence, various mechanisms of heat transfer

CONTACT Shahaboddin Shamshirband Shahaboddin.Shamshirband@tdut.edu.vn

such as convection, conduction, and radiation can take place. In fact, the increase in the in-situ reservoir temperature brings significant effects in interaction of rock-fluid which can impact the behavior of the flow (Akhlaghinia, Torabi, & Chan, 2013; Ashrafi, Souraki, & Torsaeter, 2012; Esmaeili, Sarma, Harding, & Maini, 2019a). It is worth mentioning that in addition to the presence of heat transfer mechanisms, related-multiphase phenomena such as diffusion and dispersion also make their marks in TOER. As a result, a more complicated multiphase flow in porous media is noticed when implementing TEOR techniques. The commonly applied mathematical approach to describe the flow is these cases is the outgrowth of the Darcy flow equation to multiphase flow (Maini, 1998) and thermal-based Darcy flow (Ameli et al., 2018).

Relative permeability is considered a vital factor that is involved in the mathematical models describing the multiphase flow in porous media, in which TEOR processes belong (Esmaeili, Sarma, Harding, & Maini, 2019b; Esmaeili et al., 2019a; Maini, 1998; Nait Amar et al. 2019). Relative permeability which is commonly denoted K_r, is recognized as the ratio of effective permeability of a fluid at given saturation to the absolute permeability (Ahmed, 2018). Relative permeability data are a must for a large variety of fluid flow calculations related to TEOR. As a matter of fact, modeling and simulation tasks, which are the means to forecast and predict the performances that can be achieved under different scenarios of these techniques cannot be done without the specification of the relative permeability at reservoir conditions. Hence, it is necessary to have accurate and representative values for this parameter to reduce the risks and uncertainties in the simulation results. However, it is needed to add that relative permeability can be affected by various factors and parameters, among which we can cite the absolute permeability, viscosities of water and oil phases and saturation (Honarpour, Nagarajan, & Sampath, 2006). In addition, the changes made in the fluids and rock proprieties by the temperature upsurge influence the relative permeability curves in TEOR (Casse & Ramey Jr, 1979; Ehrlich, 1970; Honarpour et al., 2006; Sinnokrot, 1969; Zhang, Tong, Xiong, & Zhao, 2017).

The temperature impact on relative permeability values and the shape of their curves has received considerable attention during last decades (Ashrafi et al., 2012; Esmaeili et al., 2019a; Maini, 1998; Zhang et al., 2017). Although unanimous agreement is not satisfied in this topic, a dominant part of experimental and modeling studies that have been published, have noticed the dependency of relative permeability in oil – water systems (Kro and Krw) on temperature (Esmaeili et al., 2019a; Esmaeili et al., 2019b; Li et al., 2014; Schembre, Tang, & Kovscek, 2005; Weinbrandt, Ramey Jr, & Casse, 1975). The investigation conducted by (Weinbrandt et al., 1975) confirmed this statement using consolidated Boise sandstone and mineral oil. The studies of (Schembre et al., 2005) and (Li et al., 2014) demonstrated the effect of temperature on the two-phase oil–water relative permeability on two distinct cases. In addition, the research performed by (Ehrlich, 1970) based on the adsorption resulted in analytical paradigm for the temperature dependency of oil–water relative permeability. Besides, some other models based on IFT as intermediate influencing parameters were developed by (Amaefule & Handy, 1982) and (Kumar, Torabzadeh, & Handy, 1985). To keep the work concise, a deep overview about different studies conducted in the literature to inspect the effect of temperature on relative permeability can be found in our prior published work (Nait Amar, Noureddine, Hemmati-Sarapardeh, & Shamshirband, 2019) and other relevant publications (Akhlaghinia et al., 2013; Ashrafi et al., 2012; Esmaeili et al., 2019a; Esmaeili et al., 2019b; Zhang et al., 2017).

Experimentally, the two-phase oil – water relative permeability in heavy oil cases can be measured by means of three possible techniques: low / high rate displacement tests; and the steady-state co-injection method (Maini, 1998). However, the experimental approaches suffer from sensitive drawbacks such as the complexity of lab preparation and realization, the long time needed to accomplish the tests without forgetting the expensive cost. Therefore, in recent years, addressing these issues by establishing cheap and simple-to-use methods to gain the impact of temperature on Kr has triggered a huge amount of scientific inquiry. (Zhang et al., 2017), (Mosavat, Mohsenzadeh, & Al-Wahaibi, 2016), (Torabi, Mosavat, & Zarivnyy, 2016), and (Bennion, Thomas, Schulmeister, & Ma, 2006) are among the well-known predictive correlations that consider the temperature influence on Kr in oil – water systems. A summary of the aforementioned correlations is given in Table 1. As it is shown in this table, although the form straightforwardness of the prior correlations, they suffer from lack of generalization as their applicability domains are limited to restricted ranges of temperature, rock and fluids parameters. In addition, it should be added that these preexisting correlations have been implemented on the basis of limited databank. In the same context, some other correlations have been established by (Esmaeili, Sarma, Harding, & Maini, 2019c), but these models are not unified with respect to the types of the rock and fluids, and hence, each of them is applicable for specific case, such as consolidated or unconsulated sands interacted with light/heavy.

Table 1. Summary of the important correlations for temperature-based oil/water relative permeability prediction. (Bennion et al., 2006), (Mosavat et al., 2016), (Torabi et al., 2016) and (Zhang et al., 2017) are.

Model	Correlations		Note
(Bennion et al., 2006)	$60^\circ C < T < 100^\circ C$	$K_{rw} = 0.021\left(1 - \frac{0.6-S_w}{0.45}\right)^5$ $K_{ro} = \left(\frac{0.6-S_w}{0.45}\right)^{2.2}$	On the basis of: • McMurray sand • Unsteady state / steady state • Heavy oil • Darcy law / history match Restrictions: • $0.11 < S_{wi} < 0.43$ • $0.12 < S_{or} < 0.72$ • $8000 < \mu_o < 10^6 cP$
	$150^\circ C < T < 275^\circ C$	$K_{rw} = 0.055\left(1 - \frac{0.85-S_w}{0.7}\right)^{2.5}$ $K_{ro} = \left(\frac{0.85-S_w}{0.7}\right)^3$	
(Torabi et al., 2016)	$K_{rw} = 0.0466\left(0.0588\frac{P_{exp}}{P_{std}}\right)^{-1.28676} \times e^{0.34443\left(2-\frac{q_{exp}}{q_{std}}\right)} \times \left(0.0025\frac{\mu_o}{\mu_{std}}\right)^{-0.34267}\left(\frac{S_w - S_{wi}}{1 - S_{wi}}\right)^2$		On the basis of: • Berea sandstone • Unsteady state approach • Heavy oil and light oil • JBN method Restrictions: • $0.092 < S_{wi} < 0.138$ • $0.463 < S_{or} < 0.539$ • $27 < T < 45^\circ C$ • $24.3 < \mu_o < 400.2 cP$
	$K_{ro} = \left(0.0588\frac{P_{exp}}{P_{std}}\right)^{-0.0291} \times e^{-0.01254\left(2-\frac{q_{exp}}{q_{std}}\right)} \times \left(1 - \frac{S_w - S_{wi}}{1 - S_{wi}}\right)^2 \times \left(1 - \left(\frac{S_w - S_{wi}}{1 - S_{wi}}\right)^{0.1\left(0.025\frac{\mu_o}{\mu_{std}}\right)^{-0.818}}\right)$		
(Mosavat et al., 2016)	$K_{rw} = \left(\frac{S_w - S_{wi}}{1 - S_{wi}}\right)^a$	$a = 1.32 + 0.00123\left(\frac{\mu_o}{\mu_w}\right) - 7.47 \times 10^{-7}\left(\frac{\mu_o}{\mu_w}\right)^2$ $b = 102 + 0.000298\left(\frac{\mu_o}{\mu_w}\right) - 1.38 \times 10^{-7}\left(\frac{\mu_o}{\mu_w}\right)^2$ $c = 2.22 + 0.00318\left(\frac{\mu_o}{\mu_w}\right) - 1.22 \times 10^{-6}\left(\frac{\mu_o}{\mu_w}\right)^2$	On the basis of: • Ottawa silica sand • Unsteady state approach • Heavy oil • History match Restrictions: • $0.05 < S_{wi} < 0.105$ • $0.2 < S_{or} < 0.413$ • $23 < T < 100^\circ C$ • $19.5 < \mu_o < 1860 cP$
	$K_{ro} = \left(1 - \left(\frac{S_w - S_{wi}}{1 - S_{wi}}\right)^b\right)\left(1 - \frac{S_w - S_{wi}}{1 - S_{wi}}\right)^c$		
(Zhang et al., 2017)	$K_{rw} = K_{rw}^{0-50C}\left(e_1 + e_2 T + \frac{e_3}{T} + \frac{e_4}{T^2}\right)\left(\frac{S_w - S_{wi}}{1 - S_{wi} - S_{or}}\right)^{a_3 T + a_4}$	$e_1 = 20.14$ $e_2 = -0.053$ $e_3 = -1638.84$ $e_4 = 40763.24$ $a_1 = 0.0244$ $a_2 = 3.8848$ $a_3 = -0.0001$ $a_4 = 0.5099$ $b_1 = 0.0025$ $b_2 = 0.1941$ $c_1 = -0.1121$ $c_2 = 0.6711$	On the basis of: • Tight sand stone • Unsteady state approach • Light oil • Combination of JBN and Corey correlation Restrictions: • $0.234 < S_{wi} < 0.482$ • $0.153 < S_{or} < 0.324$ • $25 < T < 100^\circ C$ • $4 < \mu_o < 48 cP$
	$K_{ro} = \left(\frac{1 - S_w - c_1 \ln(T) - c_2}{1 - b_1 T - b_2 - c_1 \ln(T) - c_2}\right)^{a_1 T + a_2}$		

On the other hand, smart computational techniques have emerged and evolved as powerful and advanced approaches that can resolve highly complex related-modeling topics (Amirian, Dejam, & Chen, 2018; Hemmati-Sarapardeh, Ghazanfari, Ayatollahi, & Masihi, 2016; Hemmati-Sarapardeh et al., 2018; Hobold & da Silva, 2019; Nait Amar & Zeraibi, 2018; Nait Amar, Zeraibi, & Redouane, 2018a; Nait Amar, Zeraibi, & Redouane, 2018b; Redouane, Zeraibi, & Amar, 2018; Shahsavar, Khanmohammadi, Karimipour, & Goodarzi, 2019; Xi, Gao, Xu, Zhao, & Li, 2018). Among the successful examples of soft computing techniques applications, we can cite production forcasting in thermal enhanced oil recovery (Amirian, Leung, Zanon, & Dzurman, 2015; Amirian, Fedutenko, Yang, Chen, & Nghiem, 2018), optimization of enhanced oil recovery techniques (Nait Amar & Zeraibi 2019), reservoir flood control (Chuntian & Chau, 2002), hydrology (Chau, 2017; Wu & Chau, 2011; Yaseen, Sulaiman, Deo, & Chau, 2019), and meteorology related topics (Ali Ghorbani, Kazempour, Chau, Shamshirband, & Ghazvinei, 2018; Moazenzadeh, Mohammadi, Shamshirband, & Chau, 2018).

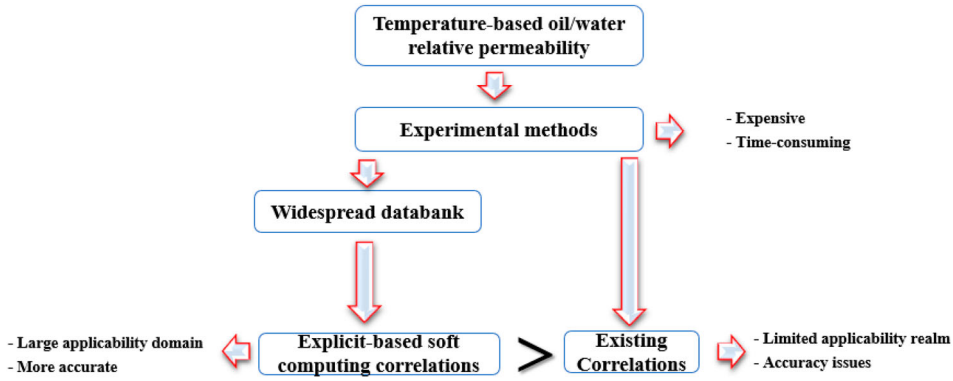

Figure 1. General sketch of the problem.

More recently, Esmaeili et al. (Esmaeili et al., 2019b) applied least square support vector machine (LSSVM) to model the dependency of oil – water relative permeability on temperature. (Nait Amar et al., 2019) proposed various intelligent paradigms as kinds of trustworthy models to estimate oil – water relative permeability in TEOR by combining radial basis function (RBF) neural network and LSSVM with some nature-inspired algorithms. The developed models in the two aforementioned studies showed very satisfactory predictions. The present investigation was done with the aim of implementing explicit, user-friendly and accurate correlations using group method of data handling (GMDH) and gene expression programming (GEP) for predicting the dependency of Kr in the two – phase oil – water systems on temperature, so that it could be applicable to a wider range of temperature, and fluids and rock proprieties.

In the present work, group method of data handling (GMDH) and gene expression programming (GEP) are applied to establish reliable correlations for estimating temperature-based oil – water relative permeability through defining five input parameters; namely the saturation of water (S_w), absolute permeability (K), temperature (T), oil and water viscosities (μ_o and μ_w). To this end, a comprehensive data source of 1223 points gathered from valid available literature and covering an extensive range of rock and fluids parameters and temperature, is utilized to establish the correlations. After developing GEP and GMDH models, they are assessed by means of several statistical criteria and graphical error analyses. Lastly, to testify the reliability of the proposed correlations, these ones are compared with pre-existing correlations that model the dependency of oil – water relative permeability on temperature. There are some important differences between the present study and the previously performed studies in literature: (1) the established paradigms in this study have widespread applicability ranges, and besides, (2) different user-friendly explicit expressions for modeling temperature dependency of Kro and Krw in thermal enhanced oil recovery processes are developed. Figure 1 recaps the sketch of the problem.

The next sections of the paper are ordered as follows. Section 2 highlights a detailed description of the databank employed to establish the correlations. Section 3 describes the GMDH and GEP concepts. Results are described and discussed in Section 4. Finally, Section 5 points out the main outcoming results.

2. Data description

To develop reliable correlations that can ensure the generalization and accuracy, a comprehensive and a large databank with widespread conditions must be considered. Due to this fact, in this study, 1223 experimental data points were collected from published literature (Akhlaghinia et al., 2013; Ashrafi et al., 2012; Ashrafi, Souraki, & Torsaeter, 2014; Lo & Mungan, 1973; Maini & Okazawa, 1987; Poston, Ysrael, Hossain, & Montgomery III, 1970; Sinnokrot, Ramey Jr, & Marsden Jr, 1971; Torabi et al., 2016; Weinbrandt et al., 1975). The collected data cove a wide range of temperature and fluid/rock conditions. Among the 1223, 648 points describe the oil relative permeability (K_{ro}) cases, while the remaining 575 correspond to the relative permeability of water (K_{rw}). The considered inputs to develop the correlations are the following: temperature (T), water saturation (S_w), water viscosity (μ_w), oil viscosity (μ_o) and the absolute permeability (K). Table 2 reports a full description of the employed databank in this study. It should be mentioned that these data have already been used in our previous paper (Nait Amar et al., 2019).

To establish the correlations using GEP and GMDH, the database was divided randomly into training data covering 80% of the whole databank, and testing data

Table 2. Statistical description of the input/output data.

			Max	Min	Mean	SD
Oil Relative Permeability	Input	Absolute permeability (mD)	95000	147	21778.9	34047.5
		Temperature (°C)	200	21.10	97.75	47.31
		S_w	1	0.052	0.4623	0.2010
		Water viscosity (cP)	1.10	0.136	0.42	0.29
		Oil viscosity (cP)	1190	0.419	88.93	224.38
	Output	K_{ro}	1	0	0.3634	0.3118
Water Relative Permeability	Input	Absolute permeability (mD)	95000	147	23443.39	35241
		Temperature (°C)	200	21.10	99.56	45.66
		S_w	1	0.052	0.533	0.219
		Water viscosity (cP)	1.10	0.136	0.40	0.27
		Oil viscosity (cP)	1190	0.7	88.39	223.19
	Output	K_{rw}	1	0	0.1096	0.2029

including the remaining 20%. The training data were used to investigate for the best correlations, while the testing data were exploited to evaluate the behavior of the correlations with blind data.

3. Models

3.1. Group method of data handling (GMDH)

Group Method of Data Handling (GMDH) known also as polynomial neural network is one of the most promising families of artificial neural networks (ANNs) (Dargahi-Zarandi, Hemmati-Sarapardeh, Hajirezaie, Dabir, & Atashrouz, 2017). Beside the reliability shown by GMDH in modeling complex systems, it ensures the advantage of providing user-friendly polynomial formula to the system being studied. The conception of GMDH technique consists in employing multiple nodes which belong to intermediate layers. The generated value by each GMDH node is calculated based on a quadratic polynomial model that includes the previous neuron. This GMDH version corresponds to the earliest model that was introduced by (Ivakhnenko, Krotov, & Ivakhnenko, 1970). As the earliest version of GMDH presented some generalization lacks, a modified version, known also as hybrid version, was proposed as an extensive version that includes more interactions between the nodes and variables; hence, this version ensures more flexibility for modeling more complex systems (Rostami et al., 2019). The GMDH hybrid version follows the below-shown rule:

$$y_i = a + \sum_{i=1}^{d}\sum_{j=1}^{d}\cdots\sum_{k=1}^{d} c_{ij\ldots k}x_i^n x_j^n \ldots x_k^n n = 1, 2, \ldots, 2^m \tag{1}$$

where $y_i, x_{ij\ldots k}$ stand for the inputs and output parameters of the model, respectively; $c_{ij\ldots k}$ denote the polynomial coefficients; m and d mean respectively, the size of layers and the input parameters number.

Afterwards, the full-form mathematical formulation can be done by partial polynomials with predefined orders to combine between the nodes in previous layers; hence, new nodal variables (i.e. O_1, O_2, ...) are created. For the case of two neurons related with a quadratic polynomial model, the following equation is applied:

$$O_i^{GMDH} = a_0 + a_1x_i + a_2x_j + a_3x_ix_j + a_4x_i^2 + a_5x_j^2 \tag{2}$$

To adjust the coefficients of the above-shown equation, the least square method (LSM) is applied. Therefore, the following expression is formulated:

$$\delta_j^2 = \sum_{i=1}^{N_t}(y_i - O_i^{GMDH})^2\, j = 1, 2, \ldots, \binom{d}{2} \tag{3}$$

In which d is the variables number and N_t is the size of the training set.

To solve this problem, this latter if transformed to a matrix form as (Dargahi-Zarandi et al., 2017; Hemmati-Sarapardeh & Mohagheghian, 2017):

$$y = A^T X \tag{4}$$

The LSM generates the solution of Eq. (4) as follows:

$$A^T = yX^T(XX^T)^{-1} \tag{5}$$

where $y = \{y_1, y_2, \ldots, y_d\}$ *and* $A = \{a_0, a_1, a_2, a_3, a_4, a_5\}$, in which d points out the number for variables.

3.2. Gene expression programming (GEP)

Gene expression programming (GEP) is an advanced soft computing method which was introduced by Ferreira (Ferreira 2001). This technique is a part of the family of evolutionary algorithms (EAs) and it applies the evolutionary principles. GEP provides the advantage of generating explicit mathematical expression to the studied systems. From the conception standing point of view, GEP is regarded an improved version of Genetic Programming

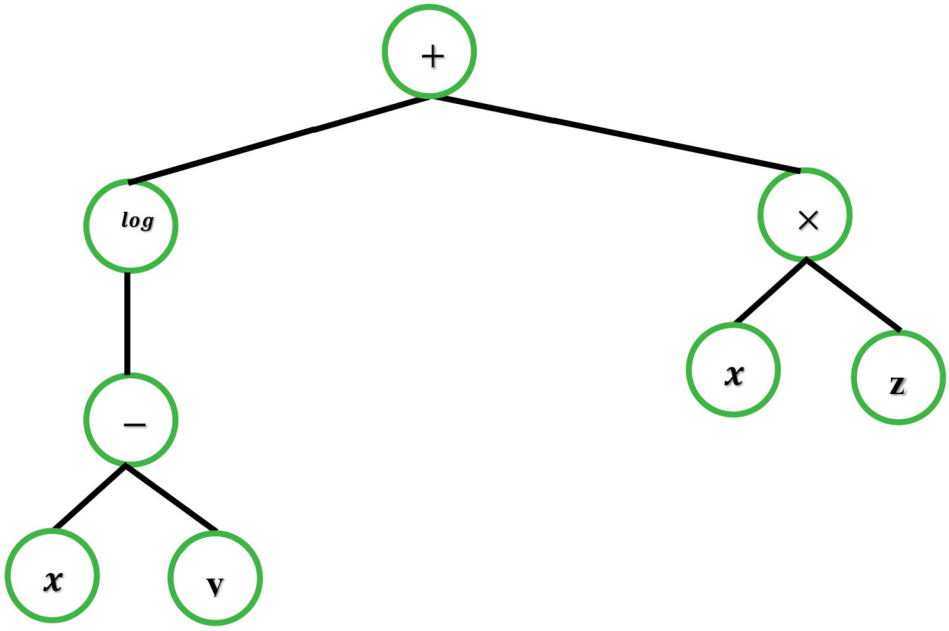

Mathematical expression: $log(x-y)+x\times z$

Figure 2. An example of two-gene chromosome and its mathematical expression.

(GP) introduced by (Koza, 1992), as GEP handled the GP issues, such as the limited regression strategies (Ferreira 2001).

As the other evolutionary algorithm, GEP processes the searching for best expression model by employing chromosomes that codify and reflect possible solutions. In addition, another key element which is the Expression Tree (ET) is introduced in GEP. ET is obtained by transforming the chromosomes into real candidates. GEP employs genes that involve terminals and a head containing functions. Each gene has a fixed length list of symbols which represent kinds of operators such as $\{+, \times, -, /, log, \sqrt{}\}$ and a terminal set such as $\{x, y, z\}$ (Teodorescu & Sherwood, 2008). Figure 2 shows a chromosome having two genes and its mathematical formula.

The GEP searching procedure is summarized in the following steps:

(1) GEP setting parameters: it consists to define the needed key parameters such as the size of the population, the stopping criteria, and the length of genes.
(2) Population initialization: create randomly initial chromosomes (different possible mathematical expression).
(3) Evaluate the chromosomes using a fitness function.
(4) Select the fittest individuals and save them for the next generation.
(5) Apply tournament selection to choose the individuals that will be recombined to generate new offspring. One point and two points recombination are available in GEP.
(6) Mutation operator: mutation plays a principal role in GEP. It changes genomes by modifying an element by another.
(7) Transposition and insertion of sequences somewhere in a chromosome: it consists to activate and jump parts of the genome in the chromosome (Ferreira 2001).

The steps from (3) to (7) are reiterated while the stopping criterion is not satisfied.

4. Results and discussion

4.1. Developing the correlations

As previously mentioned, after preparing the databank and specifying the training and testing sets for both cases Kro and Krw, the two rigorous techniques namely GEP and GMDH were applied to establish correlations for these two parameters with the following inputs: the saturation of water (S_w), absolute permeability (K), temperature (T), oil and water viscosities (μ_o and μ_w). Therefore, the temperature dependency of oil – water relative permeability correlations are developed with respect to

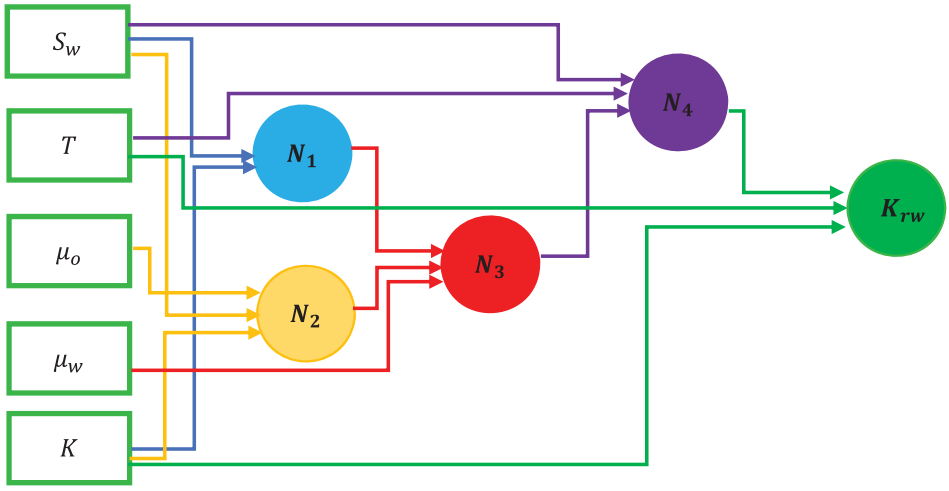

Figure 3. A schematic structure of the proposed GMDH for predicting Krw.

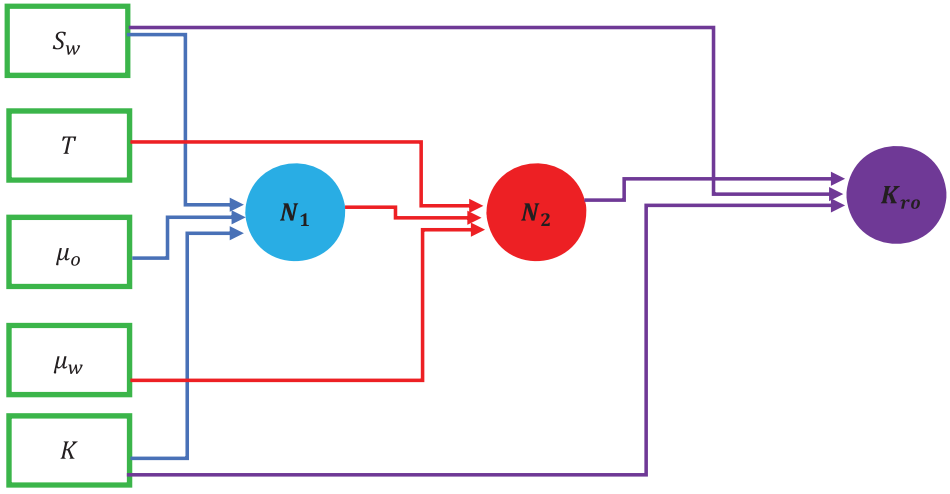

Figure 4. A schematic structure of the proposed GMDH for predicting Kro.

the aforementioned inputs as follows:

$$K_{ro} = f(S_w, T, \mu_o, \mu_w, K) \tag{6}$$

$$K_{rw} = f(S_w, T, \mu_o, \mu_w, K) \tag{7}$$

In both approaches, mean square error (MSE) was defined as the error function to be minimized during the search process for the best correlations. MSE is defined as follows:

$$MSE = \frac{\sum_1^N (Kr_{iexp} - Kr_{ipre})^2}{N} \tag{8}$$

in which Kr means the oil or water relative permeability, N is the number of points and the subscript *pre* and *exp* mean the predicted and experimental values, correspondingly.

When implementing GEP technique, its control parameters such as the population size, mutation probability, the included operators, etc. should be tuned to improve the accuracy of the generated correlations. The considered GEP setting parameters in this study are stated in Table 3.

Table 3. GEP setting parameters used in the study.

Parameters	Value/setting
The number of head size	8 – 15
Chromosome	150
Gene	8 – 12
Population	300 – 500
Mutation rate	0.25
Inversion rate	0.1
Operators used	+, −, ×, /, EXP, X^2, INV, TANH, LOG , SQRT

A summarized schematic of the K_{rw} and K_{ro} correlations obtained with GMDH are presented in Figures 3 and 4, correspondingly. As it is shown in these figures, the K_{rw} network encompasses one input layer, one output layer and three intermediate layers; while for the case of K_{ro}, one input layer, one output layer and two

intermediate layers were obtained. The resulted GMDH correlations are expressed as follows:

- K_{rw}

$$\begin{aligned} K_{rw} = {} & 0.023971 + 0.790913 \times N_4 \\ & - 4.492498 \times 10^{-7} \\ & \times K - 0.00104 \times T - 3.950588 \times 10^{-6} \\ & \times K \times N_4 - 0.000433 \times T \times N_4 \\ & + 4.465764 \times 10^{-9} \\ & \times T \times K + 0.610576 \times N_4^2 + 2.816213 \\ & \times 10^{-11} \times K^2 + 1.4329 \times 10^{-5} \times T^2 \\ & + 5.142623 \times 10^{-9} \times T \times K \times N_4 \\ & + 0.00068 \times K \times N_4^2 \\ & - 2.7281999 \times 10^{-10} \times K^2 \times N_4 + 0.002079 \\ & \times T \times N_4^2 + 2.737294 \times 10^{-13} \times T \times K^2 \\ & - 8.539067 \times 10^{-6} \times T^2 \times N_4 \\ & - 1.877768 \times 10^{-10} \\ & \times T^2 \times K - 0.58709 \times N_4^3 \\ & - 3.568052 \times 10^{-16} \\ & \times K^3 - 4.849053 \times 10^{-8} \times T^3 \end{aligned} \tag{9}$$

- K_{ro}

$$\begin{aligned} K_{ro} = {} & 0.728253 - 0.072037 \times N_2 + 3.82443 \times 10^{-5} \\ & \times K - 3.4903857 \times S_w - 1.549463 \times 10^{-5} \\ & \times K \times N_2 + 0.100212 \times S_w \times N_2 \\ & - 1.124351 \times 10^{-5} \\ & \times S_w \times K + 0.934668 \times N_2^2 \\ & - 9.736863 \times 10^{-10} \\ & \times K^2 + 5.4835969 \times S_w^2 - 3.342406 \times 10^{-5} \\ & \times S_w \times N_2 - 1.073647 \times 10^{-5} \times K \times N_2^2 \\ & + 4.3652039 \times 10^{-10} \times K^2 \times N_2 \\ & + 2.154452 \times S_w \times N_2^2 \\ & + 6.461956 \times 10^{-10} \times S_w \times K^2 \\ & + 0.8212563 \times S_w^2 \times N_2 \\ & - 3.8461259 \times 10^{-5} \times S_w^2 \times K - 0.662322 \\ & \times N_2^3 + 4.315276 \times 10^{-15} \times K^3 \\ & - 2.820277 \times S_w^3 \end{aligned} \tag{10}$$

The resulted GMDH nodes and genomes included in the above-obtained correlations are reported in Appendix A.

The obtained correlations by GEP are expressed as follows:

- K_{rw}

$$\begin{aligned} K_{rw} = {} & -(0.02353 \times S_w + 0.1717 \times S_w^2) \times K^{0.5} \\ & \times \exp(-\mu_o) - 0.0007187 + A + B + C + D \end{aligned} \tag{11}$$

where A, B, C and D are defined as shown-below:

$$\begin{aligned} A = {} & \frac{30.40 \times S_w^6}{\exp(-\mu_o) + \ln(K) - 1} \\ & - \frac{60.6 \times S_w^6}{1.759 \times (S_w^2 + \ln(K)) - 0.955} \end{aligned} \tag{12}$$

$$\begin{aligned} B = {} & -\frac{3.713 \times S_w^4}{1.126 \times (S_w^2 + \mu_w^2) - 8.898} \\ & - \frac{7.349 \times S_w^4}{45.04 \times (\mu_o + \tanh(\mu_o)) - 362.7} \end{aligned} \tag{13}$$

$$\begin{aligned} \mathrm{C} = {} & -\frac{2.123 \times 10^{-5} \times S_w^2 \times T^2}{2 \times \mu_o + \ln(K) - 17.43} \\ & - \frac{1.011 \times 10^{-3} \times S_w^4 \times \mu_o^2}{4.612 \times (\mu_o + \mu_w) + 73.63} \end{aligned} \tag{14}$$

$$D = -\frac{29.92 \times S_w \times \exp(-S_w^2) \times \sqrt{\exp(-\mu_o)}}{T} \tag{15}$$

- K_{ro}
- − For $21.10 < T \leq 100^{\circ}C$

$$\begin{aligned} K_{ro} = {} & 0.05447 \left(\frac{S_w \times T \times \mu_o}{K} \right) (0.12071 \times T - 1) \\ & + 0.04403 \left(\sqrt{\frac{K}{\mu_w}} \right) \left(\frac{0.2376}{\sqrt{\mu_w}} - 1 \right) \\ & + \mu_o \left(0.00619 + \frac{17.9}{T - K} \right) + A_1 \times S_w - A_2 \\ & \times (S_w \times T \times \mu_w) - A_3 \times \left(\frac{\mu_w}{T} \right) \\ & + A_4 \times \left(\frac{K}{S_w} \right) - A_5 + A_6 \end{aligned} \tag{16}$$

−For $100 < T \leq 200^{\circ}C$

$$\begin{aligned} K_{ro} = {} & 0.7083 \times S_w^2 \times \left(0.003467 \times T \times \sqrt{\mu_o} - S_w^4 \right) \\ & + 10^{-6} \times \Big[7834 \times \mu_w^3 - 5.963 \times \left(T^2 + \sqrt{\mu_o} \right) \end{aligned}$$

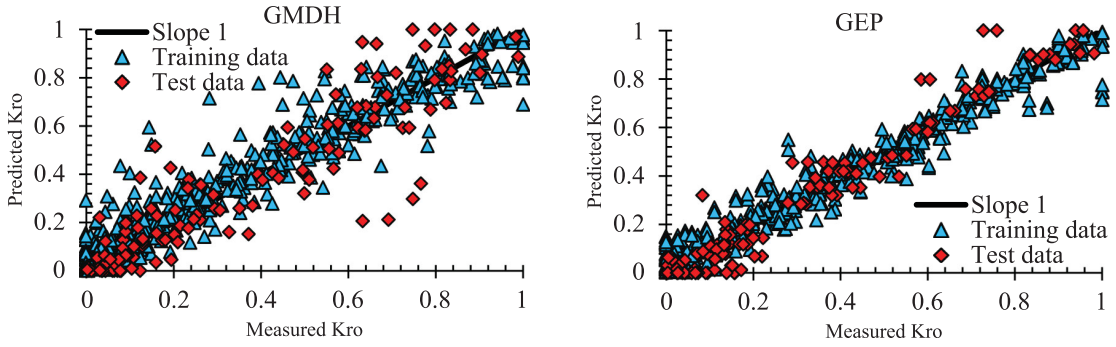

Figure 5. Cross plots of the established GMDH and GEP correlations (Kro).

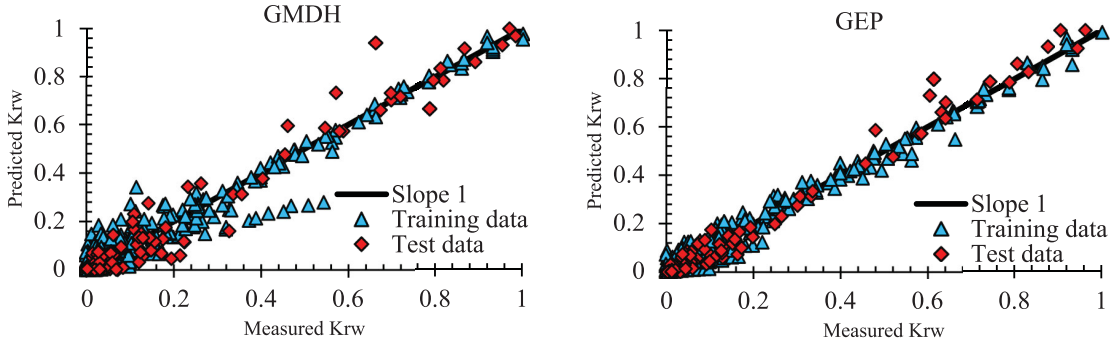

Figure 6. Cross plots of the established GMDH and GEP correlations (Krw).

$$+ A_1 \times (S_w \times K) + A_2 \left(\frac{K}{T}\right) - A_3 \left(\frac{K}{\mu_w}\right) + A_4 \times \mu_o^{\frac{3}{2}} - \frac{A_5}{\sqrt{S_w}}\Bigg] + A_6 \times \mu_o + A_7 \qquad (17)$$

The expressions of the terms appearing in the obtained GEP correlation for Kro are specified in Table 4.

4.2. Performances evaluation

Graphical error analyses and statistical criteria and were employed to assess the accuracy of the developed correlations and chose the best representative ones in forecasting the temperature – based K_{ro} and K_{rw}.

The root mean square error (RMSE) and coefficient of determination (R^2) and are the statistical indexes that were used in this study. These two statistical criteria are defined in Appendix B.

To fine-tune the above-mentioned criteria, broaden the assessment of the established correlations and give visual comparisons, graphical evaluation diagrams such as cross plots, and histograms of error distribution were considered. In the cross plots, the predicted values by the correlations are plotted versus the counterpart

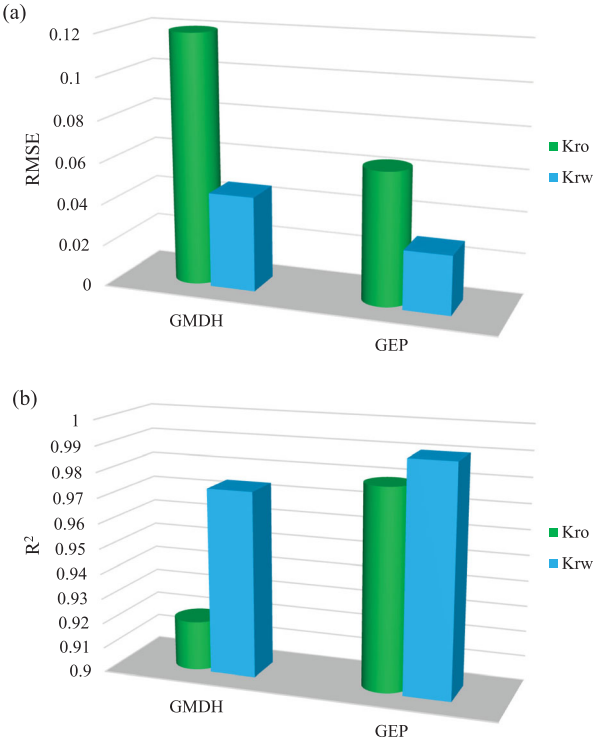

Figure 7. Comparison between the established correlations: (a) RMSE and (b) R^2.

Table 4. Expressions of the terms appearing in Kro GEP correlations.

	$21.10 < T \leq 100^{\circ}C$	$100 < T \leq 200^{\circ}C$
A_1	$0.5492 \times \mu_w + 3.596 \times S_w - \frac{10^{-5} \times T^2}{1.3 \times \mu_o - 10.67562}$	$5.8 - 6.343 \times S_w \times \sqrt{\mu_o}$
A_2	$0.06567 + 0.1093 \times \tanh(\mu_w) - 0.001972 \times S_w \times T \times \mu_w + \left(\frac{S_w}{K}\right) \times (0.467 \times T + 3.869)$	$7422 \times S_w - 4659 \times \tanh(S_w) - 5.8 \times T$
A_3	$0.4542 + \mu_w(0.001875 \times K + 0.007486) + \frac{0.0003327 \times K}{\mu_w}$	$11.01 + \frac{1.809}{\mu_w}(T - 1)$
A_4	$\frac{1.355 \times 10^{-5}}{T \times \mu_w^2} - \frac{6.954 \times 10^{-6}}{\sqrt{\mu_o}}$	$68.06 + 6.343 \times S_w^2$
A_5	$0.6238 \times \exp(2 \times S_w) + 0.3137 \ln(T + \mu_o) + (4.421 - 0.02517 \times \ln(K)) \times \ln(K)$	$7.523 \times (T + K) + \frac{11.01 \times \mu_o}{\sqrt{S_w}}$
A_6	$0.006523 \times \left(\sqrt{K} - \mu_w\right) + \frac{0.0001183 \times (K - T)}{\mu_o} + 27.8$	$-0.007834 + \frac{2.722}{K} + \frac{0.3102 \times S_w \times \mu_w}{3.603 \times \mu_o - 30.37}$
A_7		$\frac{0.03168 + 0.009715 \times \mu_o}{\tanh(\mu_w)} - 4.208 \times \tanh(\tanh(S_w))$ $+0.6253 \times \ln(S_w + \mu_w) + 2.722 \times \sqrt{\mu_w} - 1.437 \times \mu_o^{\frac{1}{4}} + 2.702$

Table 5. Statistical indexes of the established correlations.

		Training		Testing		All	
		RMSE	R^2	RMSE	R^2	RMSE	R^2
K_{rw}	GMDH	0.0468	0.9711	0.0408	0.9846	0.0456	0.9738
	GEP	0.0278	0.9899	0.0305	0.9918	0.0284	0.9903
K_{ro}	GMDH	0.1206	0.9221	0.1296	0.9104	0.1224	0.9197
	GEP	0.0610	0.9809	0.0740	0.9737	0.0636	0.9794

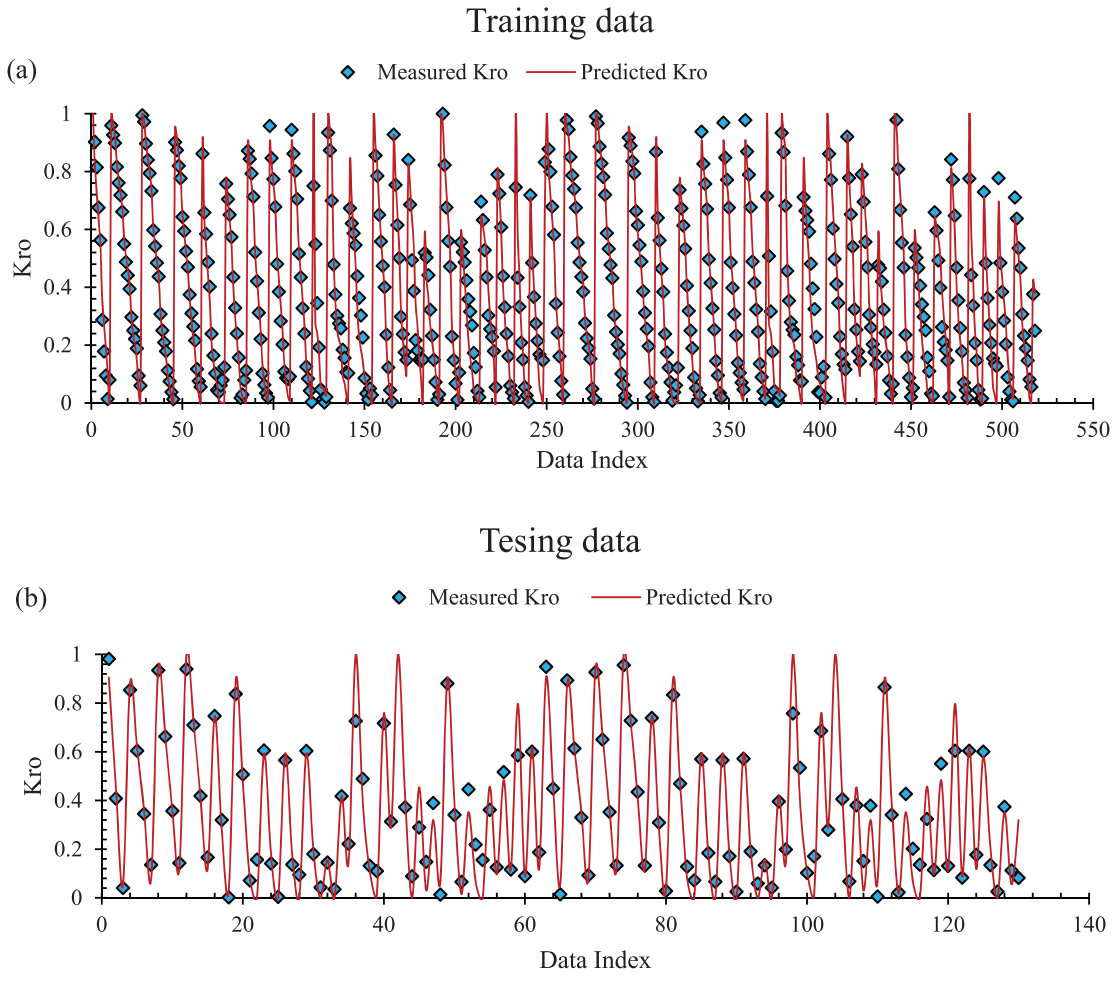

Figure 8. The comparison between the predicted Kro values by the GEP model and the Kro real values: (a) training data and (b) testing data.

experimental values. Existence of large amount of points nearby the line Y = X indicated the high accuracy of the model and the excellent degree of correspondence between predictions and real data. In the histograms of error, the distribution of errors is plotted in a bar form and if a normal distribution is noticed nearby zero value, the model is deemed very satisfactory.

Figures 5 and 6 display cross plots comparing between experimental data and predictions of GEP and GMDH correlations for Kro and Krw, respectively. As it can be obviously seen from these figures, GMDH predictions show large sparse for both Kro and Krw, whereas the predictions of GEP are accumulated nearly enough around the unit slope line. According to this visual survey, it can be said that the GEP correlations are more awe-inspiring as sublime accommodations between their predictions and experimental results are noticed. To excavate the integrity of the established correlations and distinguish the most representative one, Table 5 and bar plots of Figure 7 report statistical and graphical error analyses through the considered assessment criteria, namely RMSE and R^2, for the established correlations. With

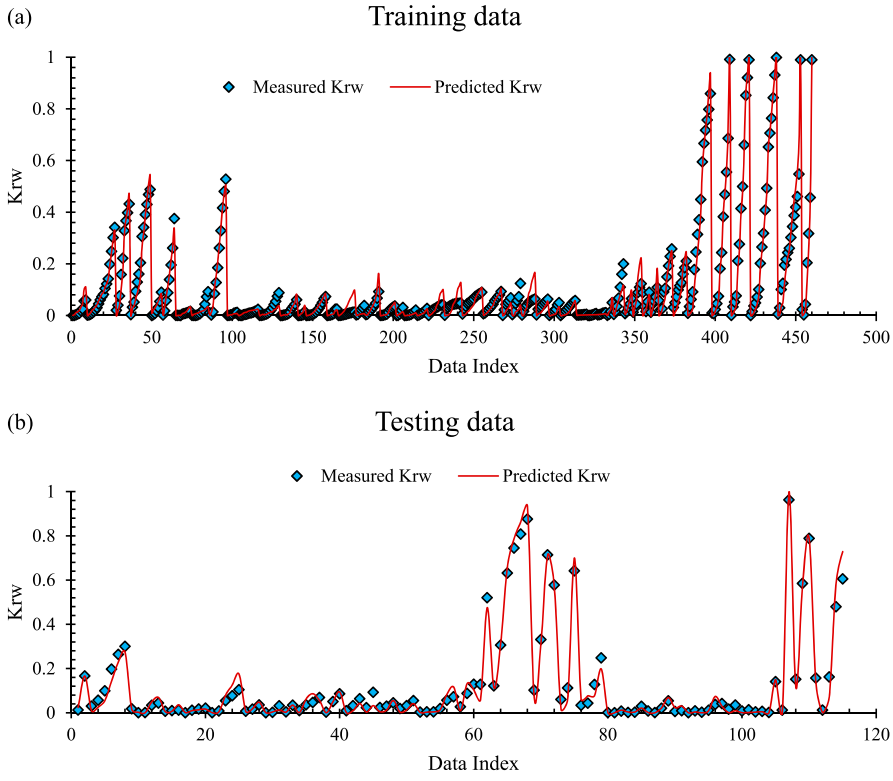

Figure 9. The comparison between the predicted Krw values by the GEP model and the Krw real values: (a) training data and (b) testing data.

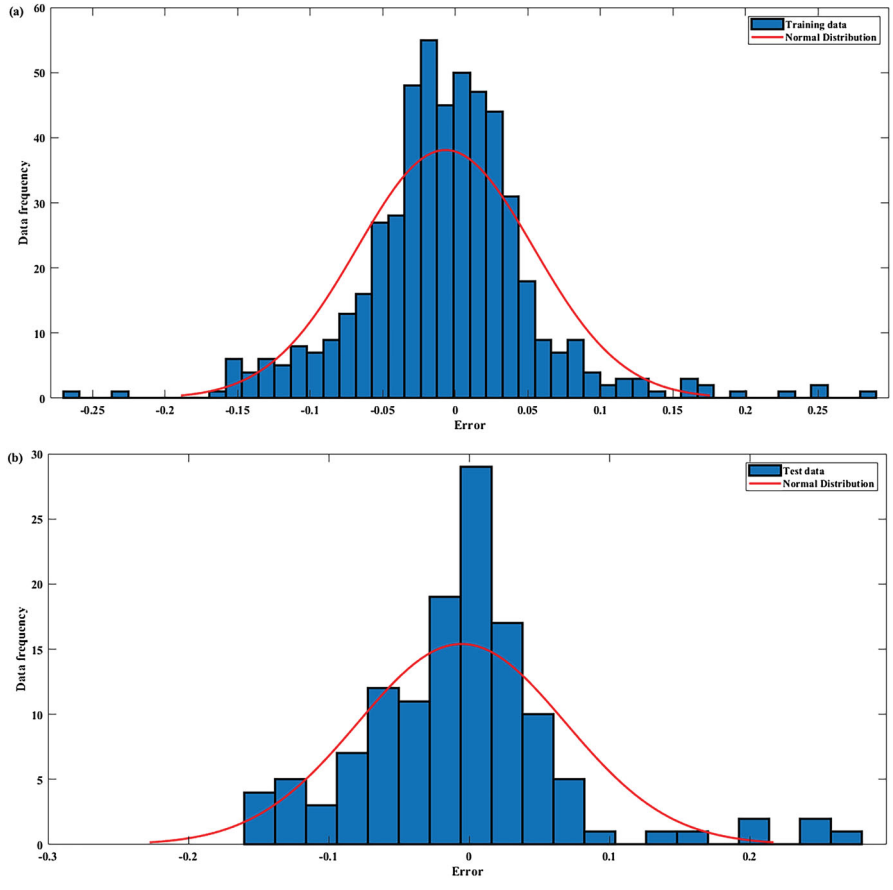

Figure 10. Histogram plot for the datasets applied in establishing GEP correlation for Kro: (a) train and (b) test.

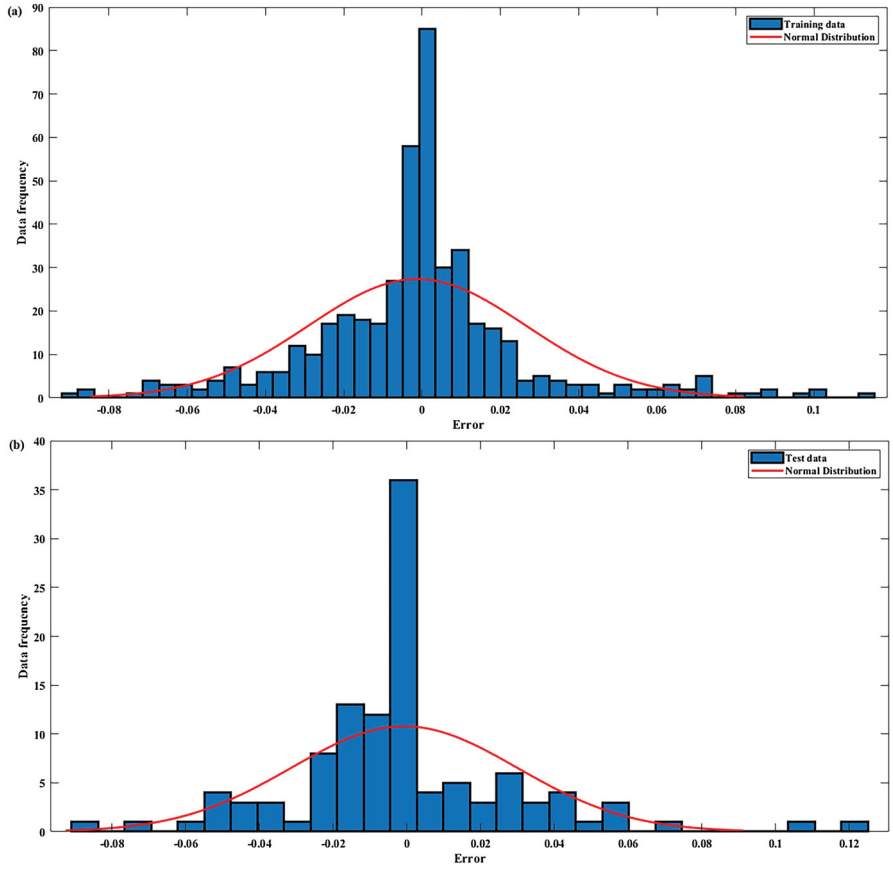

Figure 11. Histogram plot for the datasets applied in establishing GEP correlation for Krw: (a) train and (b) test.

accordance to the demonstrated results in Table 5 and Figure 7, it can be concluded that GEP correlations estimate better K_{rw} and K_{ro} compared to GMDH correlations. The temperature-based oil – water relative permeability correlations established using GEP exhibit overall RMSE values of 0.0284 and 0.0636 for K_{rw} and K_{rw}, respectively, and correlation coefficients that exceed 0.97 for the both cases. Therefore, the developed GEP correlations were considered for further investigation in the rest of paper.

To depict effectiveness and reliability of the GEP correlations regarded to the generated results, the comparison between predicted relative permeability from the implemented correlations and their counterpart real values versus corresponding indexes of data samples were demonstrated in Figure 8 for Kro and in Figure 9 for Krw. As these figures illustrate, the gained results from the GEP correlations are as close as possible to actual values of Krw and Kro during the training and testing phases.

For a better understanding of the GEP correlations integrity in estimating the temperature – based Kro and Krw, Figures 10 and 11 demonstrate histograms of errors between the actual and estimated values for Kro and Krw, respectively. These figures include error histograms for training and testing phases in the two cases, Kro and Krw.

Table 6. Statistical parameters of various models for temperature-based oil-water relative permeability.

		RMSE	R^2
K_{ro}	Mosavat et al.	0.2982	0.8257
	Zhang et al.	0.1879	0.8326
	Bennion et al.	0.2665	0.6240
	GEP	0.0636	0.9794
K_{rw}	Mosavat et al.	0.3105	0.7687
	Zhang et al.	0.0451	0.8923
	Bennion et al.	0.2425	0.2347
	GEP	0.0284	0.9903

Based on the reported results in these histograms, we can observe that the most frequent error values are nearby zero. In addition, it can be said that the error distributions follow the normal curve in all the subplots. The error distributions reported in Figures 10 and 11 confirm the high ability of the established correlations in predicting the temperature – based Kro and Krw.

4.3. Comparison of developed GEP correlations with literature models

In the present study, the accuracy of the developed GEP correlations was compared to various available correlations in the literature, which include the effect of

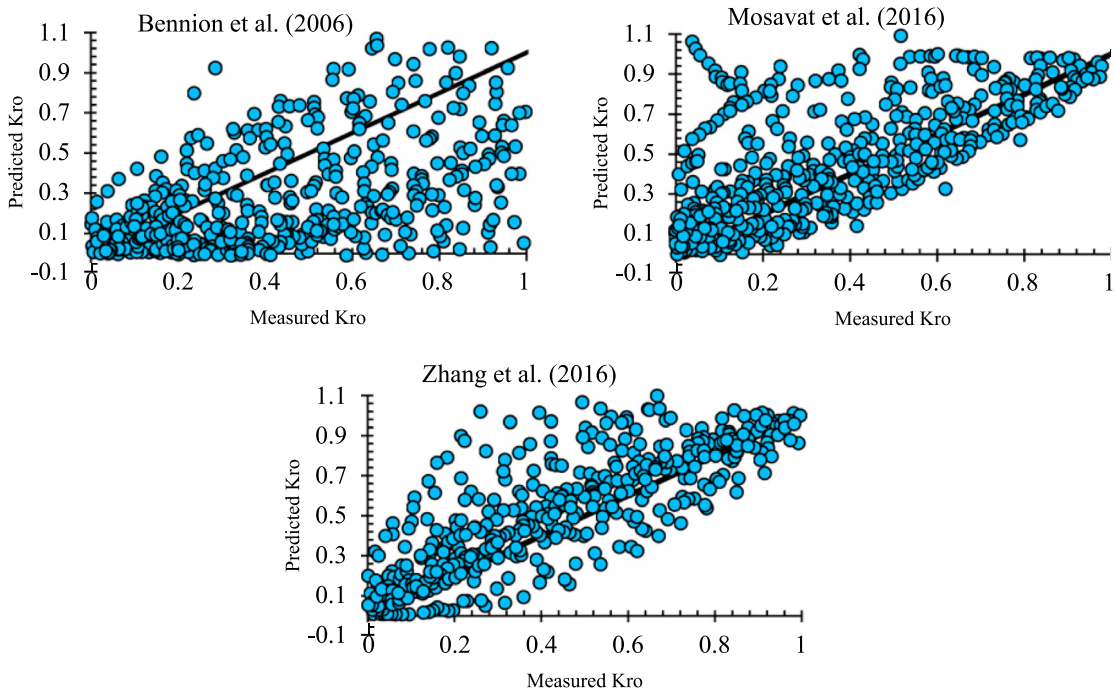

Figure 12. Comparison of experimental and predicted temperature-based oil relative permeability by Bennion et al., Mosavat et al. and Zhang et al.

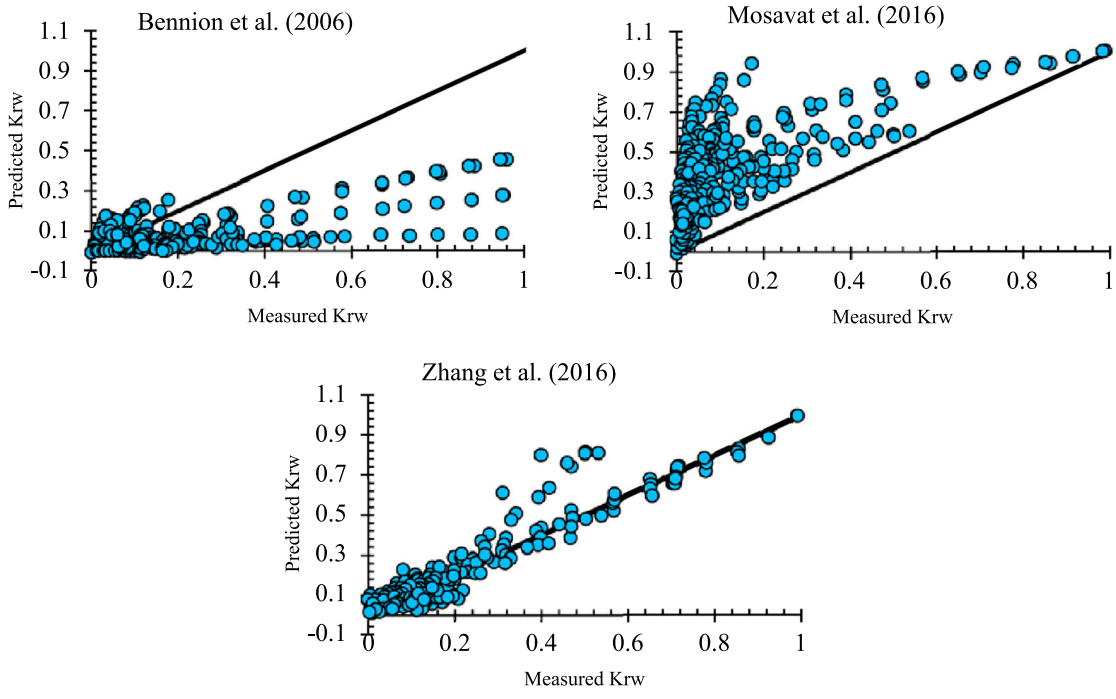

Figure 13. Comparison of experimental and predicted temperature-based water relative permeability by Bennion et al., Mosavat et al. and Zhang et al.

temperature on Kro and Krw. These latter include (Bennion et al., 2006), (Zhang et al., 2017), and (Mosavat et al., 2016). It should be mentioned that while applying the preexisting correlations to the employed data in this study, only the points that fall within the application ranges were included according to each correlation. To this end, the estimated values using the previously mentioned correlations versus the experimental data are

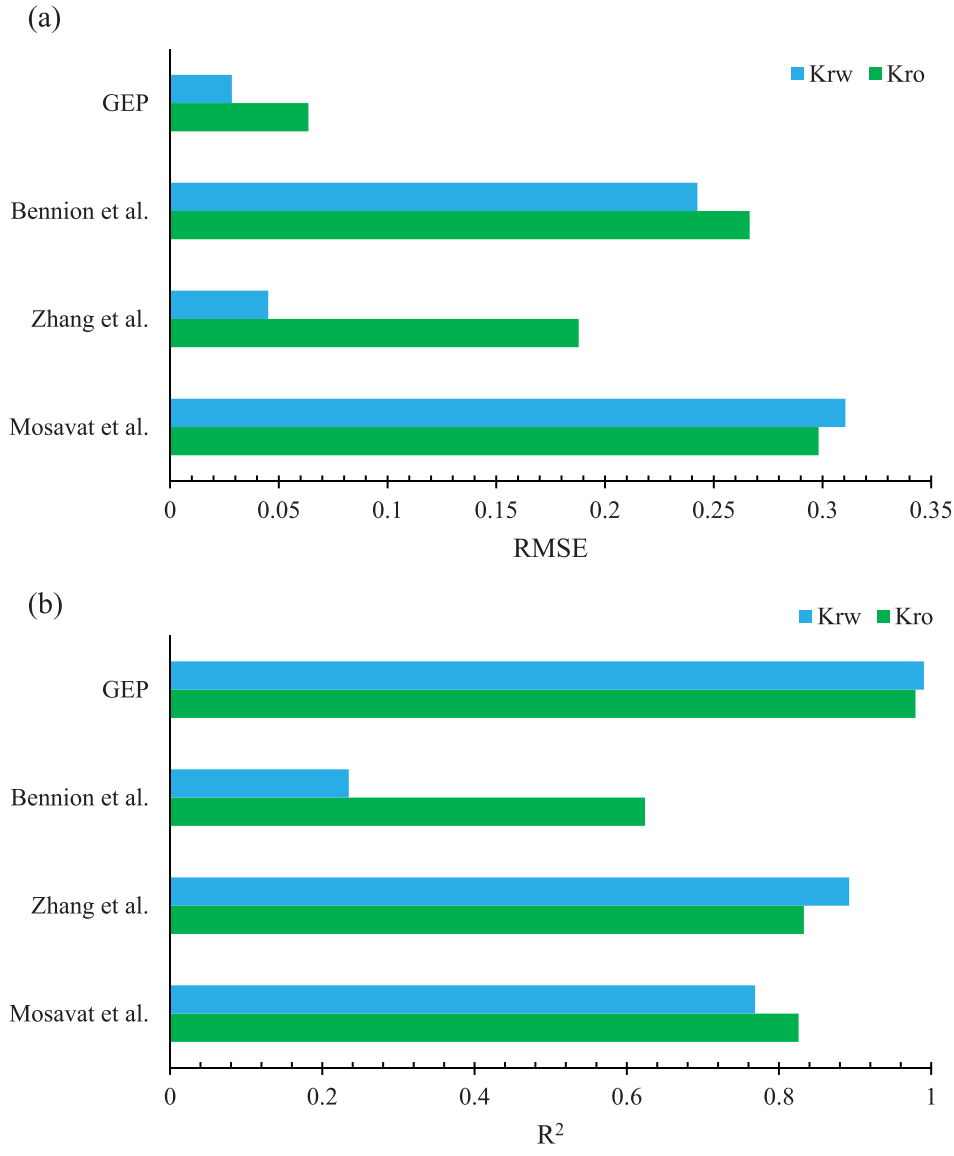

Figure 14. The obtained (a) root mean squared error and (b) coefficient of correlation while estimating temperature-based oil/water relative permeability by GEP and available pre-existing correlations.

plotted in Figure 12 for Kro and in Figure 13 for Krw. Figures 12 and 13 demonstrate that large scatters in the Kro and Krw data around the unit slop line were generated by (Bennion et al., 2006) and (Mosavat et al., 2016) correlations, while acceptable accumulation around the X = Y line was noticed in the case of estimating Krw with the (Zhang et al., 2017) correlation. This obviously indicates that (Bennion et al., 2006) and (Mosavat et al., 2016), correlations fail in forecasting the correct values of both Kro and Krw, whereas (Zhang et al., 2017) fails particularly in predicting Kro.

Table 6 and Figure 14 summarize the performances of the correlations considered in this work along with those of GEP correlations. The comparison results show that the developed GEP correlations lead to the best performances in predicting both Kro and Krw. According to Table 6 and Figure 14, it is concluded that the developed GEP correlations outperforms largely the preexisting temperature-based oil/water correlations.

4.4. Validity of the developed GEP correlations in term of water saturation (S_w)

To testify the efficiency of the established GEP correlations in predicting the curves of temperature – based Kro and Krw as function of S_w, Figure 15 illustrates the generated Kro and Krw curves via GEP correlations, and compare with corresponding experimental values from two different samples included in this study. As the subplots (a) and (b) of Figure 15 depict, a very satisfactory integrity is shown by the GEP correlations to estimate the temperature-based Kro and Krw curves as their emulated

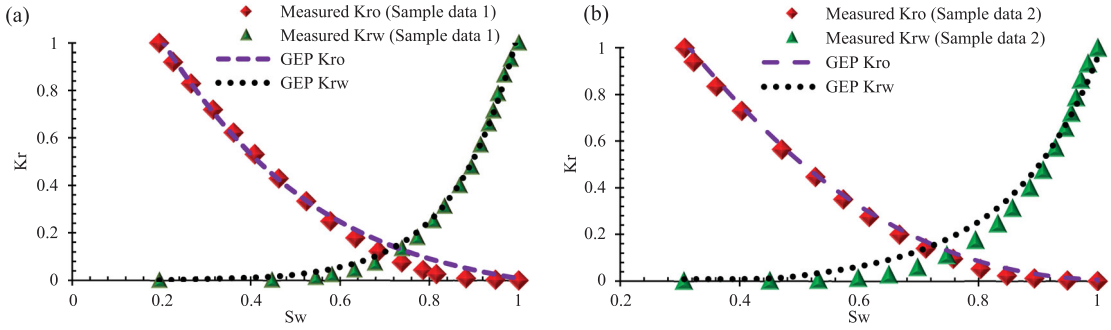

Figure 15. Comparison between experimental values and outputs generated via GEP correlations versus water saturation for two cases included in this study.

results have almost identical behaviors as actual records do. The prediction capability of the proposed GEP correlations has once again been certified in Figure 15.

Finaly, it should be mentioned that the proposed correlation for modeling the temperature dependency of Kro and Krw should be utilized when the data falls within the applicability realm, otherwise its exactness is not ensured as precise results for certain conditions can be generated, and imprecise results for some others. However, as previously stated, these correlations were gained by including widespread databank, and hence, it can be applied for several cases which have input parameters filling in the applicability realm.

5. Conclusions

In this study, new explicit, simple-to-use and accurate correlations were proposed to model the dependency of relative permeability in oil – water systems on temperature. Group method of data handling (GMDH) and gene expression programming (GEP) were implemented as promising tools to implement the correlations using a large comprehensive databank. Several assessment criteria were considered to figure out integrity and performance of the new correlations. The main conclusions of the study are summarized as follows:

1. GEP-based correlations were found as the most reliable correlations to predict the temperature dependency of Kr in oil – water relative systems.
2. The newly implemented GEP correlations for predicting the temperature-based Kro and Krw exhibited very satisfactory performances with overall RMSE values of 0.0284 and 0.0636 for Krw and Kro, respectively.
3. The developed GEP correlations were compared with other well-known preexisting correlations; namely those of (Zhang et al., 2017), (Bennion et al., 2006) and (Mosavat et al., 2016). The integrity of the proposed correlations was testified and found to be substantially superior to all of these models.
4. By performing a trend analysis of the developed GEP correlations in term of water saturation, the gained curves for both Kro and Krw followed the expected forms and logical variations in term of water saturation.
5. The established correlations in this study can be applied under a wide variety of conditions and also can be improved in presence of new additional data.

Nomenclature

Acronyms

ANNs	artificial neural networks
CSS	cyclic steam stimulation
GEP	gene expression programming
GMDH	group method of data handling
IFT	interfacial tension
LSSVM	least square support vector machine
MSE	mean square error
RBFNN	radial basis function neural network
RMSE	Root mean squared error
R^2	coefficient of determination
SAGD	steam-assisted gravity drainage
TEOR	thermal enhanced oil recovery

Variables

K	absolute permeability
K_{ro}	oil relative permeability
K_{rw} water	relative permeability
S_w	water saturation
T	temperature
μ_w	water viscosity
μ_o	oil viscosity

Subscripts

Min	minimum
Max	maximum

Disclosure statement

No potential conflict of interest was reported by the authors.

References

Ahmed, T. (2018). *Reservoir engineering handbook*. Houston: Gulf Professional Publishing.

Akhlaghinia, M., Torabi, F., & Chan, C. W. (2013). Effect of temperature on two-phase relative permeabilities of heavy oil, water, carbon dioxide, and methane determined by displacement technique. *Energy & Fuels*, *27*(3), 1185–1193.

Ali Ghorbani, M., Kazempour, R., Chau, K.-W., Shamshirband, S., & Ghazvinei, P. T. (2018). Forecasting pan evaporation with an integrated artificial neural network quantum-behaved particle swarm optimization model: A case study in Talesh, Northern Iran. *Engineering Applications of Computational Fluid Mechanics*, *12*(1), 724–737.

Amaefule, J. O., & Handy, L. L. (1982). The effect of interfacial tensions on relative oil/water permeabilities of consolidated porous media. *Society of Petroleum Engineers Journal*, *22*(03), 371–381.

Ameli, F., Alashkar, A., & Hemmati-Sarapardeh, A. (2018). Thermal Recovery Processes.

Amirian, E., Dejam, M., & Chen, Z. (2018). Performance forecasting for polymer flooding in heavy oil reservoirs. *Fuel*, *216*, 83–100.

Amirian, E., Fedutenko, E., Yang, C., Chen, Z., & Nghiem, L. (2018). Artificial neural network modeling and forecasting of oil reservoir performance. In *Applications of data management and analysis* (pp. 43–67). Cham: Springer.

Amirian, E., Leung, J. Y., Zanon, S., & Dzurman, P. (2015). Integrated Cluster analysis and artificial neural network modeling for steam-assisted gravity drainage performance prediction in heterogeneous reservoirs. *Expert Systems with Applications*, *42*(2), 723–740.

Ashrafi, M., Souraki, Y., & Torsaeter, O. (2012). Effect of temperature on athabasca type heavy oil–water relative permeability curves in Glass Bead Packs. *Energy and Environment Research*, *2*(2), 113–126.

Ashrafi, M., Souraki, Y., & Torsaeter, O. (2014). Investigating the temperature dependency of oil and water relative permeabilities for heavy oil systems. *Transport in Porous Media*, *105*(3), 517–537.

Bennion, D. B., Thomas, F. B., Schulmeister, B., & Ma, T. (2006). A Correlation of the Low and High Temperature Water-Oil Relative Permeability Characteristics of Typical Western Canadian Unconsolidated Bitumen Producing Formations. In *Canadian International Petroleum Conference*.

Casse, F. J., & Ramey Jr, H. J. (1979). The effect of temperature and confining pressure on single-phase flow in consolidated rocks (includes associated paper 9087). *Journal of Petroleum Technology*, *31*(08), 1–51.

Chau, K.-w. (2017). Use of meta-heuristic techniques in rainfall-runoff modelling. *Water*, *9*(3), 186–192.

Chuntian, C., & Chau, K.-W. (2002). Three-person multi-objective conflict decision in reservoir flood control. *European Journal of Operational Research*, *142*(3), 625–631.

Dargahi-Zarandi, A., Hemmati-Sarapardeh, A., Hajirezaie, S., Dabir, B., & Atashrouz, S. (2017). Modeling gas/vapor viscosity of hydrocarbon fluids using a hybrid GMDH-Type neural network system. *Journal of Molecular Liquids*, *236*, 162–171.

Ehrlich, R. (1970). The effect of temperature on water-oil imbibition relative permeability. In *SPE Eastern Regional Meeting*.

Esmaeili, S., Sarma, H., Harding, T., & Maini, B. (2019a). Review of the effect of temperature on oil-water relative permeability in porous rocks of oil reservoirs. *Fuel*, *237*, 91–116.

Esmaeili, S., Sarma, H., Harding, T., & Maini, B. (2019b). A data-driven model for predicting the effect of temperature on oil-water relative permeability. *Fuel*, *236*, 264–277.

Esmaeili, S., Sarma, H., Harding, T., & Maini, B. (2019c). Correlations for effect of temperature on oil/water relative permeability in clastic reservoirs. *Fuel*, *246*, 93–103.

Ferreira, C. (2001). Algorithm for Solving gene expression programming: A new adaptive problems. *Complex Systems*, *13*(2), 87–129.

Green, D. W., & Paul Willhite, G. (1998). *Enhanced Oil Recovery*. Vol. 6. Henry L. Doherty Memorial Fund of AIME, Society of Petroleum Engineers Richardson, TX.

Hemmati-Sarapardeh, A., Ameli, F., Varamesh, A., Shamshirband, S., Mohammadi, A. H., & Dabir, B. (2018). Toward generalized models for estimating molecular weights and acentric factors of pure chemical compounds. *International Journal of Hydrogen Energy*, *43*(5), 2699–2717.

Hemmati-Sarapardeh, A., Ghazanfari, M.-H., Ayatollahi, S., & Masihi, M. (2016). Accurate determination of the CO2-crude oil minimum miscibility pressure of pure and impure CO2 streams: A robust modelling approach. *The Canadian Journal of Chemical Engineering*, *94*(2), 253–261.

Hemmati-Sarapardeh, A., & Mohagheghian, E. (2017). Modeling interfacial tension and minimum miscibility pressure in paraffin-nitrogen systems: Application to gas injection processes. *Fuel*, *205*, 80–89.

Hobold, G. M., & da Silva, A. K. (2019). Automatic detection of the onset of film boiling using convolutional neural networks and bayesian statistics. *International Journal of Heat and Mass Transfer*, *134*, 262–270.

Honarpour, M. M., Nagarajan, N. R., & Sampath, K. (2006). Rock/fluid characterization and their integration—implications on reservoir management. *Journal of Petroleum Technology*, *58*(09), 120–130.

Ivakhnenko, A. G., Krotov, G. I., & Ivakhnenko, N. (1970). Theoretical Systems Ecology: Advances and Case Studies.

Koza, J. R. (1992). *Genetic programming II, Automatic Discovery of Reusable Subprograms*. Cambridge, MA: MIT Press.

Kumar, S., Torabzadeh, S. J., & Handy, L. L. (1985). Relative Permeability Functions for High-and Low-Tension Systems at Elevated Temperatures. In *SPE California Regional Meeting*.

Li, B., Pu, W. F., Li, K. X., Jia, H., Wang, K. Y., & Yang, Z. G. (2014). The characteristics and Impacts factors of relative permeability curves in high temperature and Low-permeability Limestone reservoirs. In *Advanced Materials Research* (Vol. 1010, pp. 1676–1683). Trans Tech Publications.

Lo, H. Y., & Mungan, N. (1973). Effect of temperature on water-oil relative permeabilities in oil-wet and water-wet systems. In *Fall Meeting of the Society of Petroleum Engineers of AIME*.

Maini, B. (1998). Is it futile to measure relative permeability for heavy oil reservoirs? *Petroleum Society of Canada*. doi:10.2118/98-04-06

Maini, B. R. I. J. B., & Okazawa, T. (1987). Effects of temperature on heavy oil-water relative permeability of sand. *Petroleum Society of Canada*. doi:10.2118/87-03-03

Nait Amar, M., & Zeraibi, N. (2019). An Efficient methodology for multi-objective optimization of water alternating CO2 EOR process. *Journal of the Taiwan Institute of Chemical Engineers*, *99*, 154–165.

Meyer, R. F., Attanasi, E. D., & Freeman, P. A. (2007). Heavy oil and natural bitumen resources in geological basins of the world: U.S. Geological Survey Open-File Report 2007-1084, available online at http://pubs.usgs.gov/of/2007/1084/.

Moazenzadeh, R., Mohammadi, B., Shamshirband, S., & Chau, K.-w. (2018). Coupling a firefly algorithm with support vector regression to predict evaporation in Northern Iran. *Engineering Applications of Computational Fluid Mechanics*, *12*(1), 584–597.

Mosavat, N., Mohsenzadeh, A., & Al-Wahaibi, Y. (2016). Estimating oil/water relative permeability at SAGD steam chamber edge. In *SPE Heavy Oil Conference and Exhibition*.

Nait Amar, M., Noureddine, Z., Hemmati-Sarapardeh, A., & Shamshirband, S. (2019). Modeling temperature-based oil-water relative permeability by integrating advanced intelligent models with grey wolf optimization: Application to thermal enhanced oil recovery processes. *Fuel*, *242*, 649–663.

Nait Amar, M., Zeraibi, N., & Redouane, K. (2018a). Optimization of WAG process using dynamic proxy, genetic algorithm and ant colony optimization. *Arabian Journal for Science and Engineering*, *43*(11), 6399–6412.

Nait Amar, M., Zeraibi, N., & Redouane, K. (2018b). Bottom hole pressure estimation using hybridization neural networks and grey wolves optimization. *Petroleum*, *4*(4), 419–429.

Nait Amar, M., & Zeraibi, N. (2018). Application of hybrid support vector regression artificial bee colony for prediction of MMP in CO2-EOR process. *Petroleum*. doi:10.1016/j.petlm.2018.08.001

Olayiwola, S. O., & Dejam, M. (2019). A comprehensive Review on interaction of nanoparticles with low salinity water and surfactant for enhanced oil recovery in sandstone and carbonate reservoirs. *Fuel*, *241*, 1045–1057.

Poston, S. W., Ysrael, S., Hossain, A. K. M. S., & Montgomery III, E. F. (1970). The effect of temperature on irreducible water saturation and relative permeability of unconsolidated sands. *Society of Petroleum Engineers Journal*, *10*(02), 171–180.

Prats, M. (1982). *Thermal recovery*. New York, NY: SPE of AIME.

Redouane, K., Zeraibi, N., & Amar, M. N. (2018). Automated optimization of well placement via adaptive space-filling surrogate modelling and evolutionary algorithm. In *Abu Dhabi International Petroleum Exhibition & Conference*.

Rostami, A., Hemmati-Sarapardeh, A., Karkevandi-Talkhooncheh, A., Husein, M. M., Shamshirband, S., & Rabczuk, T. (2019). Modeling heat capacity of ionic liquids using group method of data handling: A hybrid and structure-based approach. *International Journal of Heat and Mass Transfer*, *129*, 7–17.

Saboorian-Jooybari, H., Dejam, M., & Chen, Z. (2016). Heavy oil polymer flooding from laboratory core floods to pilot tests and field applications: Half-century studies. *Journal of Petroleum Science and Engineering*, *142*, 85–100.

Schembre, J. M., Tang, G.-q., & Kovscek, A. R. (2005). Effect of temperature on relative permeability for heavy-oil diatomite reservoirs. In *SPE Western Regional Meeting*.

Shahsavar, A., Khanmohammadi, S., Karimipour, A., & Goodarzi, M. (2019). A Novel comprehensive experimental study concerned synthesizes and prepare liquid paraffin-Fe3O4 mixture to develop models for both thermal conductivity & viscosity: A New approach of GMDH type of neural network. *International Journal of Heat and Mass Transfer*, *131*, 432–441.

Sinnokrot, A. A. (1969). The effect of temperature on capillary pressure curves of limestone and sandstones [Ph.D. Dissertation]. Stanford University.

Sinnokrot, A. A., Ramey Jr, H. J., & Marsden Jr, S. S. (1971). Effect of temperature level upon capillary pressure curves. *Society of Petroleum Engineers Journal*, *11*(01), 13–22.

Teodorescu, L., & Sherwood, D. (2008). High energy Physics Event selection with gene expression programming. *Computer Physics Communications*, *178*(6), 409–419.

Tillerson, R. W. (2008). Meeting Global Energy Supply and Demand Challenges. In *19th World Petroleum Congress*.

Torabi, F., Mosavat, N., & Zarivnyy, O. (2016). Predicting heavy oil/water relative permeability using modified Corey-based correlations. *Fuel*, *163*, 196–204.

Weinbrandt, R. M., Ramey Jr, H. J., & Casse, F. J. (1975). The effect of temperature on relative and absolute permeability of sandstones. *Society of Petroleum Engineers Journal*, *15*(05), 376–384.

Wu, C. L., & Chau, K. W. (2011). Rainfall–runoff modeling using artificial neural network coupled with singular spectrum analysis. *Journal of Hydrology*, *399*(3–4), 394–409.

Xi, L., Gao, J., Xu, L., Zhao, Z., & Li, Y. (2018). Study on heat transfer performance of steam-cooled ribbed channel using neural networks and genetic algorithms. *International Journal of Heat and Mass Transfer*, *127*, 1110–1123.

Yaseen, Z. M., Sulaiman, S. O., Deo, R. C., & Chau, K.-W. (2019). An enhanced extreme Learning machine model for river flow forecasting: State-of-the-art, practical applications in water resource engineering area and future research direction. *Journal of Hydrology*, *569*, 387–408.

Zhang, L.-h., Tong, J., Xiong, Y., & Zhao, Y.-l. (2017). Effect of temperature on the oil–water relative permeability for sandstone reservoirs. *International Journal of Heat and Mass Transfer*, *105*, 535–548.

Appendices

Appendix A. Obtained GMDH nodes and genomes for Kro and Krw

The resulted GMDH nodes and genomes are expressed as follows:

- Krw

$$\begin{aligned}N_4 = &-0.102767 - 1.983942 \times N_3 + 0.005098 \times T \\ &- 0.141932 \times S_w + 0.01020 \times T \times N_3 \\ &+ 6.158718 \times S_w \times N_3 - 0.006264 \times S_w \times T \\ &+ 3.078813 \times N_3^2 - 4.478272 \\ &\times 10^{-5} \times T^2 + 0.931513 \\ &\times S_w^2 - 0.010119 \times S_w \times T \times N_3 + 0.0011847 \\ &\times T \times N_3^2 - 1.530084 \times 10^{-5} \times T^2 \times N_3 \\ &+ 0.031735 \times S_w \\ &\times N_3^2 + 2.267592 \times 10^{-5} \times S_w \times T^2 - 4.639188 \\ &\times S_w^2 \times N_3 + 0.003083 \times S_w^2 \times T - 1.635732 \times N_3^3 \\ &+ 1.164436 \times 10^{-5} \times T^3 - 0.7844912 \times S_w^3\end{aligned}$$

$$\begin{aligned}N_3 = &0.176662 - 1.940022 \times N_2 + 1.3582468 \times N_1 \\ &- 0.9801913 \times \mu_w + 183.489858 \times N_1 \times N_2 \\ &+ 0.500095 \times N_2 \times \mu_w + 4.220132 \times \mu_w \times N_1 \\ &- 42.4369441 \times N_2^2 - 141.8141161 \times N_1^2 + 1.637756 \\ &\times \mu_w^2 - 235.2853497 \times \mu_w \times N_1 \times N_2 \\ &- 635.636686 \times N_1 \times N_2^2 + 545.98779 \times N_1^2 \\ &\times N_2 + 79.564658 \\ &\times \mu_w \times N_2^2 + 153.550115 \times \mu_w \times N_1^2 + 2.097266 \\ &\times \mu_w^2 \times N_2 - 4.2657881 \\ &\times \mu_w^2 \times N_1 + 225.747117 \\ &\times N_2^3 - 134.334663 \times N_1^3 - 0.891422 \times \mu_w^3\end{aligned}$$

$$\begin{aligned}N_2 = &-0.096002 - 5.9257567 \times 10^{-6} \times K - 0.000564 \\ &\times \mu_o + 1.130989 \times S_w + 3.481102 \times 10^{-9} \\ &\times \mu_o \times K - 3.823397 \times 10^{-6} \times S_w \times K \\ &- 3.6069041 \times 10^{-6} \times S_w \times \mu_o \\ &+ 2.674233 \times 10^{-10} \times K^2 \\ &+ 1.561068 \times 10^{-6} \times \mu_o^2 - 2.949632 \times S_w^2 \\ &+ 1.131077 \times 10^{-9} \times \mu_o \times K \times S_w \\ &- 4.770877 \times 10^{-14} \times \mu_o \\ &\times K^2 + 2.038109 \times 10^{-11} \times \mu_o^2 \times K \\ &+ 1.599609 \times 10^{-10} \times S_w \times K^2 \\ &- 3.171396 \times 10^{-7} \times S_w \times \mu_o^2 \\ &- 1.538897 \times 10^{-5} \times S_w^2 \times K + 0.000121 \times S_w^2 \\ &\times \mu_o - 2.397819 \times 10^{-15} \times K^3 \\ &- 9.193278 \times 10^{-10} \times \mu_o^3 + 2.792131 \times S_w^3\end{aligned}$$

$$\begin{aligned}N_1 = &-0.086648 - 6.263036 \times 10^{-6} \times K + 0.943031 \\ &\times S_w - 2.686239 \times 10^{-6} \times S_w \times K + 2.763862 \\ &\times 10^{-10} \times K^2 - 2.593159 \times S_w^2 + 1.533535 \times 10^{-10} \\ &\times S_w \times K^2 - 1.5880239 \times 10^{-5} \\ &\times S_w^2 \times K - 2.461926 \times 10^{-15} \times K^3 + 2.596955 \times S_w^3\end{aligned}$$

- Kro

$$\begin{aligned}N_2 = &-10.615467 + 3.079713 \times N_1 + 37.847865 \times \mu_w \\ &+ 0.123872 \times T - 10.501635 \times \mu_w \times N_1 \\ &- 0.038680 \times T \times N_1 - 0.266058 \times T \times \mu_w \\ &+ 4.219898 \times N_1^2 - 41.718917 \times \mu_w^2 - 0.000483 \times T^2 \\ &+ 0.067595 \times T \times \mu_w \times N_1 - 1.5338197 \times \mu_w \\ &\times N_1^2 + 7.0341954 \times \mu_w^2 \times N_1 - 0.0146348 \times T \times N_1^2 \\ &+ 0.0940588 \times T \times \mu_w^2 + 0.000135 \times T^2 \times N_1 \\ &+ 0.000562 \times T^2 \times \mu_w - 1.465284 \times N_1^3 + 15.521063 \\ &\times \mu_w^3 + 5.4498556 \times 10^{-7} \times T^3\end{aligned}$$

$$\begin{aligned}N_1 = &1.000296 - 9.2675342 \times 10^{-6} \times K - 0.000537 \\ &\times \mu_O + 0.091314 \times S_w - 7.968958 \times 10^{-8} \times \mu_O \\ &\times K - 1.500484 \times 10^{-5} \times S_w \times K - 0.001163 \\ &\times S_w + 1.466523 \times 10^{-10} \times K^2 \\ &- 9.665598 \times 10^{-7} \times \mu_O^2 \\ &- 3.759212 \times S_w^2 - 3.849348 \times 10^{-8} \times S_w \times \mu_O \\ &\times K + 1.066838 \times 10^{-12} \times \mu_O \times K^2 \\ &+ 1.416735 \times 10^{-10} \\ &\times \mu_O^2 \times K - 4.666963 \times 10^{-11} \times S_w \times K^2 \\ &+ 8.735882 \times 10^{-9} \times S_w \times \mu_O^2 \\ &+ 2.5344757 \times 10^{-5} \times S_w^2 \times K \\ &+ 0.001674 \times S_w^2 \times \mu_O - 5.754639 \times 10^{-16} \\ &\times K^3 + 9.856402 \times 10^{-10} \times \mu_O^3 + 2.665978 \times S_w^3\end{aligned}$$

Appendix B. Statistical criteria

These two assessment criteria are defined as follows:

$$R^2 = 1 - \frac{\sum_{i=1}^{N} (Kr_{ipred} - Kr_{iexp})^2}{\sum_{i=1}^{N} (Kr_{ipred} - \overline{Kr})^2}$$

$$RMSE = \sqrt{\frac{1}{N} \sum_{i=1}^{N} (Kr_{iexp} - Kr_{ipred})^2}$$

In these equations, N corresponds to the number of data, Kr_i and $\overline{Kr}$ are the phase (oil / water) relative permeability and their corresponding averages, correspondingly; and the subscripts *pred and exp* mean the predicted and experimental values, correspondingly.